

AN ANALYSIS OF A LONG-LIVED MCV OBSERVED OVER THE SOUTHERN PLAINS USING POTENTIAL VORTICITY DIAGNOSTICS

Anthony R. Lupo, Patrick S. Market, Stephen E. Mudrick,
Christopher W. Ratley, Matthew D. Chambers, and Christopher C. Rayburn

Department of Soil and Atmospheric Sciences
University of Missouri-Columbia
Columbia, Missouri

Abstract

On the morning of 28 May 1998, a mesoscale convectively-generated vortex (MCV) was observed over the Southern Plains. This MCV was evident in the GOES-8 visual satellite imagery resulting in a spectacular picture. An analysis of this event is offered using many data sources, including products available now via the World Wide Web (WWW), the NOAA/NWS National Centers for Environmental Prediction (NCEP) re-analyses, and Eta model initializations. This MCV developed out of a mesoscale convective system (MCS) that existed during 26 and 27 May over Texas. This MCV was associated with reports of severe weather and heavy precipitation over southern Arkansas. While the MCV is shown to have characteristics similar to other MCV events documented, this event is unique in that it maintained its character, while propagating further east than other events. A dynamical analysis using potential vorticity diagnostics (PV) shows that the mid-latitude vorticity field strengthened at least partially as a result of diabatic heating. Also, the most severe weather was associated with high values of integrated 500 - 300 hPa PV values over the Southern Plains.

1. Introduction

Mesoscale vortices, or mesovortices, have been shown to occur in tropical, mid-latitude (e.g., Menard and Fritsch 1989; Zhang 1992; de Coning et al. 1998), and polar (e.g., Businger and Reed 1989; Gallee 1995) flow regimes. They have also been shown to be generated by a variety of forcing mechanisms including convection (e.g., Zhang and Fritsch 1988), varying terrain (e.g., Levinson and Banta 1995), and vortex tube tilting and stretching (e.g., Weisman 1993). Mesoscale convectively-generated vortices (MCVs) are small-scale, short-lived, inertially stable, mid-level vortices that are generated in association with mesoscale convective complexes (MCCs) (e.g., Maddox 1980; Maddox et al. 1986) and mesoscale convective systems (MCSs). Johnston (1981) first documented these vortices using satellite imagery. The dynamic characteristics of MCVs have recently been studied both observationally (e.g., Menard and Fritsch 1989; Bartels and Maddox 1991; de Coning et al. 1998) and using mesoscale models (e.g., Zhang and Fritsch 1987, 1988). Although MCVs are generally of smaller scale than the current observational network, the above studies have

shown that these vortices have a warm-core structure. Also, while the forecasting of MCCs and their associated phenomena have improved in recent years, these phenomena can still make weather forecasting, especially on the local level, a more difficult task.

The goal of the following discussion is to perform a dynamical analysis, using potential vorticity (PV) diagnostics, of an MCV that occurred during 27 - 29 May 1998 over the Southern Plains. The analysis will show that the 500-hPa PV associated with the MCV intensified at least partially as a result of mid-level diabatic heating (e.g., latent heat release), and that certain PV quantities can be associated with the most severe weather in this MCV. This mid-level generation occurrence is associated with low-level PV generation due to diabatic heating. Thus, these quantities have potential for use as operational forecasting tools, since diabatic heating at mid-levels may indicate the presence of deep convection and this convection has an impact on the local PV, wind, and mass fields. Then, given a forecast map showing the local strengthening of a PV maximum, this information can be used to infer the wind and mass fields as well as the likelihood of future convection.

2. Data and Methodology

a. Data

The initial data set used for the larger-scale analysis in this investigation was the NOAA/NWS/National Centers for Environmental Prediction (NCEP) and National Center for Atmospheric Research (NCAR) re-analyses, and these are available from the NCAR mass-storage facility. The NCEP re-analyses (Kalnay et al. 1996) used here are the 2.5 degree by 2.5 degree latitude/longitude gridded analyses available on 17 mandatory levels (from 1000 to 10 hPa) at six-hour intervals. These analyses include standard atmospheric variables such as geopotential height, temperature, relative humidity, model-calculated vertical motions (ω), and u and v components, and various surface fields and tropopause information. Mandatory pressure-level data were interpolated quadratically in $\ln(p)$ to 21 isobaric levels in 50-hPa increments from 1050 to 50 hPa. The source of data used for the smaller-scale analyses were the Eta model initial fields archived at NCEP and acquired from the National Weather Service Forecast Office in Saint Charles, Missouri. Many of the same fields found in the

NCEP re-analyses are available using the Eta analyses, except that the horizontal resolution is 48 km. Finally, other data sources used in this study included GOES-8 visible satellite imagery¹, upper-air Eta model analyses from NCEP², NEXRAD radar imagery³, and the Daily Weather Map series available through NCEP.

b. Methodology

A useful quantity for examining mid-latitude phenomena in a simple and concise manner is potential vorticity (e.g., Uccellini 1976; Hoskins and Berrisford 1988; Moore 1993; Neilsen-Gammon and Lefevre 1996). Ertel (1942) derived an elegant form of this quantity from the primitive equations:

$$P = \frac{\omega_a \cdot \nabla_\theta \theta}{\rho} \quad (1)$$

where P is Ertel's potential vorticity (EPV), ω_a is the three-dimensional absolute vorticity vector, ρ is the density of air, θ is the potential temperature, and ∇_θ is the three-dimensional gradient operator on theta surfaces. For adiabatic and frictionless motion, i.e., for $d\theta/dt = 0$, we have,

$$\frac{dP}{dt} = 0 \quad (2)$$

This form of the PV has some powerful characteristics in that the EPV is conserved on surfaces of potential temperature in hydrostatic, inviscid, and adiabatic three-dimensional flows (see Pedlosky 1987). Under these conditions, an examination of (1) reveals that the dynamic and thermodynamic properties of the atmosphere are contained in one variable P . Additionally, as described by Hoskins et al. (1985), the global distribution of PV, given a suitable boundary condition and 'reference' state, can be used to determine, or recover, all the relevant dynamical fields such as winds, temperature, and pressure. This powerful property is referred to by Hoskins et al. (1985) as the 'invertability principle' for potential vorticity.

Equation (2) is a formal statement of the conservation property of PV. Also, if all dynamic and thermodynamic information is included in one variable P , then 'traditional' quasi-geostrophic atmospheric forcing, as represented by, for example, vorticity advection or temperature advection, is represented in both (1) and (2). Thus, these forcing mechanisms would represent "conservative" forcing. If (1) were conserved, provided that the atmosphere is adiabatic, then diabatic forcing, such as latent heat

release, sensible heating/cooling, or radiative heating/cooling, would represent a source or sink of potential vorticity. Sources and sinks of PV would represent non-conservative forcing.

de Coning et al. (1998) examine an MCV event over southern Africa using isentropic analysis. In their study, they examined pressure and PV distributions on θ surfaces. In this study, an MCV over North America is examined by looking at PV distributions on pressure surfaces as well. Since the current observational network uses pressure and height as the vertical coordinate, the techniques used by de Coning et al. (1998) and described above must still be acquired by vertical interpolation. Thus, calculations of PV on θ surfaces are still only approximations of the real PV fields (Hoskins et al. 1985). However, Bosart and Lackmann (1995) and Lupo and Bosart (1999) demonstrate that PV fields on pressure surfaces are useful quantities even though the conservation property is sacrificed. This relationship is defined as (see Bosart and Lackmann 1995):

$$PV = g \left(\hat{k} \cdot \left(\frac{\partial V}{\partial p} \times \nabla \theta \right) + \zeta_a \frac{\partial \theta}{\partial p} \right) \quad (3)$$

where ζ_a is the vertical component of absolute vorticity, V is the horizontal wind vector, g is the gravitation constant, and the gradient operator is a two-dimensional operator on a pressure surface. Despite the fact that PV values in (3) are no longer conserved, there is a high degree of similarity between PV calculated on theta surfaces or pressure surfaces (see Lupo and Bosart 1999; their Fig. 8).

3. Synoptic Discussion

On the morning of 28 May 1998, an initial examination of the GOES-8 Visible satellite imagery (*regional images*) revealed the spectacular image shown in Fig. 1 (1545 UTC 28 May 1998). At first glance, this mesoscale feature has an almost hurricane-like appearance. However, upon closer inspection of satellite imagery and archived Eta model analyses (not shown), it was apparent that this feature was generated as a result of strong convection that occurred on the night of 26–27 May, over western Texas. While the appearance of such an event as pictured in Fig. 1 is unusual, MCVs have been documented in the past (e.g., Velasco and Fritsch 1987; Menard and Fritsch 1989, *hereafter* MF89; Bartels and Maddox 1991). In fact, MF89 studied a similarly occurring MCV that occurred over the same area of the United States during July 1982.

As in the MF89 study, the MCV in Fig. 1 was relatively large and long-lived, the cloud shield having a diameter of roughly 400 km, covering much of the state of Arkansas at the time. The time scale for the lifecycle of the vortex (MCV) as a recognizable feature was about 30 hours when determined using the satellite imagery. However, using upper-air Eta model analyses (Fig. 2) a strong maximum in the 500-hPa absolute vorticity field

¹GOES 8 imagery was obtained from the UCAR weather processor available on the Internet at www.rap.ucar.edu/weather/.

²Eta model initial fields archived at NCEP were plotted at and obtained from the UNISYS weather processor archived on the Internet at weather.UNISYS.com/archive/eta_init/.

³The radar imagery was made available through WSI Corporation on the Internet at www.wsicorp.com

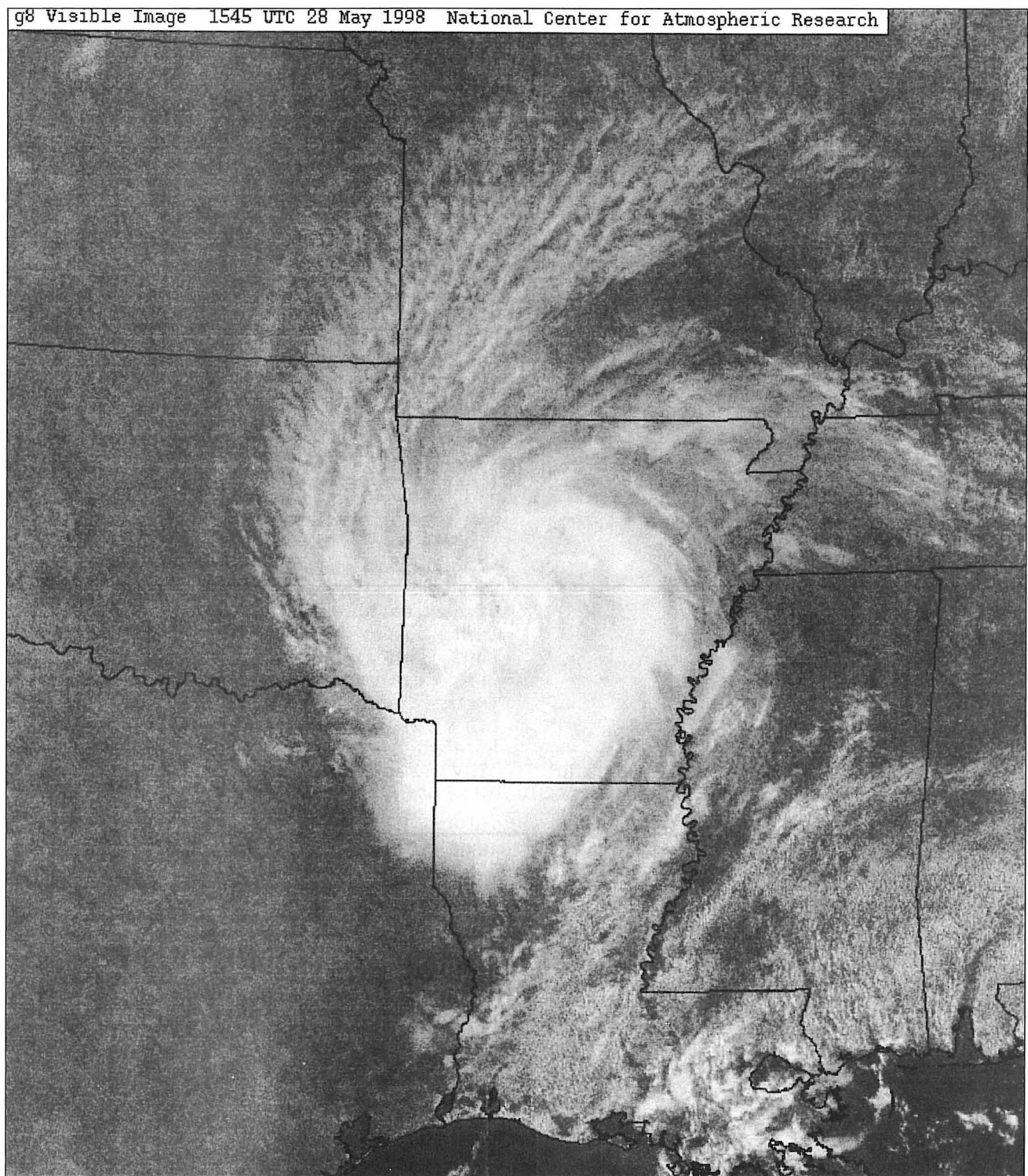


Fig. 1. A regional GOES-8 visible satellite image of the southern plains for 1545 UTC 28 May 1998.

was present starting from 1200 UTC 27 May 1998 (not shown) over Texas. This vorticity maximum remained a coherent structure until 0000 UTC 30 May, or for approximately 60-h, and continued to propagate eastward such that the vortex was over the Mississippi-Alabama border at that time.

A sample plot using the Eta model fields is shown in Fig. 2 for 0000 UTC (a), and 1200 UTC 28 May (b); Fig.

2b represents the time period closest to that in Fig. 1. The vorticity maximum associated with the MCV is the maximum located near Arkansas. Note also corresponding regions of compensating low and negative absolute vorticity located to the west and south of the vortex over the north central Texas and the Louisiana coast, respectively. While a coherent 500-hPa absolute vorticity maximum persisted for about 60-h, the clearly-defined circulation in

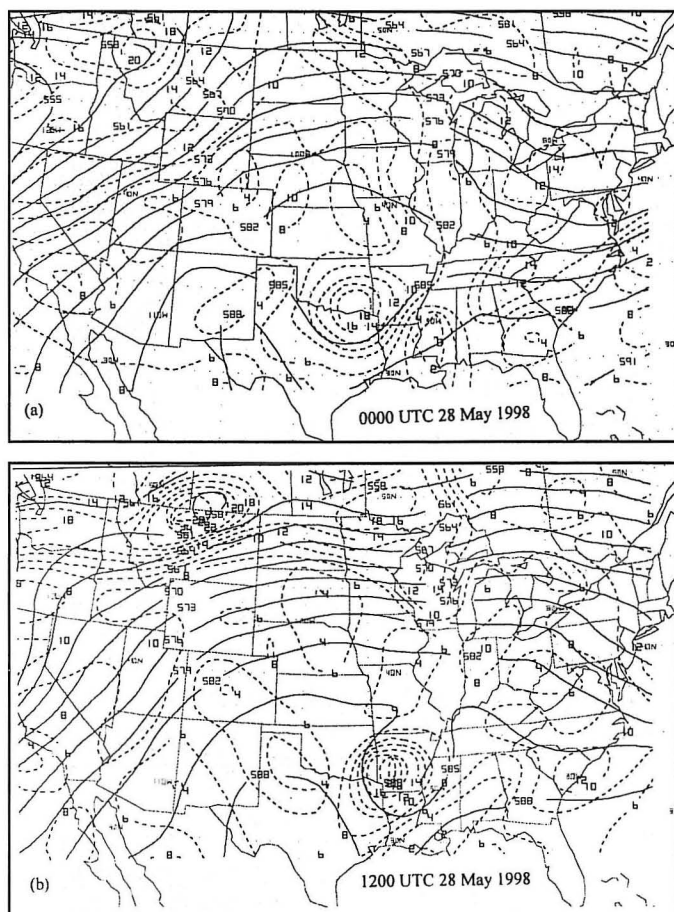


Fig. 2. The 500-hPa Eta model initialized fields from a) 0000 UTC 28 May 1998, and b) 1200 UTC 28 May 1998. Heights (solid, m) are contoured every 30 m and absolute vorticity (dashed, $1 \times 10^5 \text{ s}^{-1}$) every 2 units.

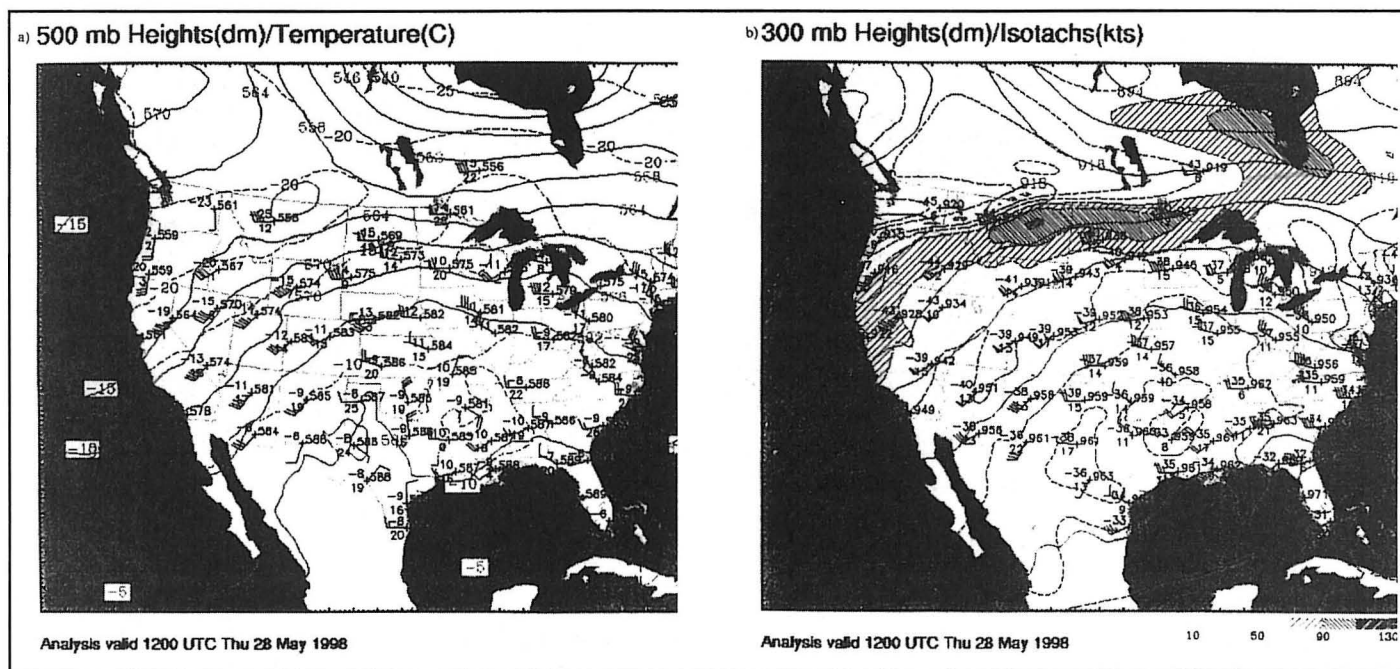


Fig. 3. The observed a) 500-hPa heights (m, contoured every 60m) and temperatures (K, 5K), and b) 300-hPa heights (m, 120m), temperatures (K, 5K), and isotachs (kts, 20 kts - starting with 10 kts) for 1200 UTC 28 May 1998. Both panels also display the rawinsonde information, and in b) wind speeds greater than 70 kts are shaded.

the satellite image (Fig. 1) was only visible for about 24-h. MF89 showed that the convection associated with these vortices has a strong diurnal cycle, strengthening during the day and weakening at night. The convection associated with this MCV event behaved similarly, although it did not result in a similar appearance on satellite imagery as seen in Fig. 1. Additionally, this MCV exhibited more eastward movement than the MCV event in MF89, which did not propagate far from the location where the MCC that spawned the event occurred. This may partially be due to the prevalence of a more zonal large-scale flow regime over the northern and mid-western United States at the steering levels (700 hPa and 500 hPa) for this event than in the MF89 case. Examining the 500-hPa PV advection field (not shown) showed that negative PV advection values (corresponding to height falls; see Lupo and Bosart 1999) were consistently downstream of the vortex. Finally, the vorticity associated with this event began to disperse on 31 May (not shown) over the southeast United States.

An examination of the upper-air charts associated with this event (Fig. 3) shows that this MCV occurred in a similar large-scale environment (within ridging flow) to that described in MF89. As was the case for their MCV event, the 850-hPa warm air advection (not shown) and the 300-hPa cyclonic vorticity advection within the local environment were both relatively weak. Note that in Fig. 3b the upper-level jet maxima were located far to the north near the US-Canadian border. A surface front was also located far to the west at 1200 UTC 28 May over western Texas, stretching north into western Nebraska (not shown). However, unlike the MF89 event, it is not apparent that the upper-level flow associated with this MCV was strongly diffluent. The winds at all levels were

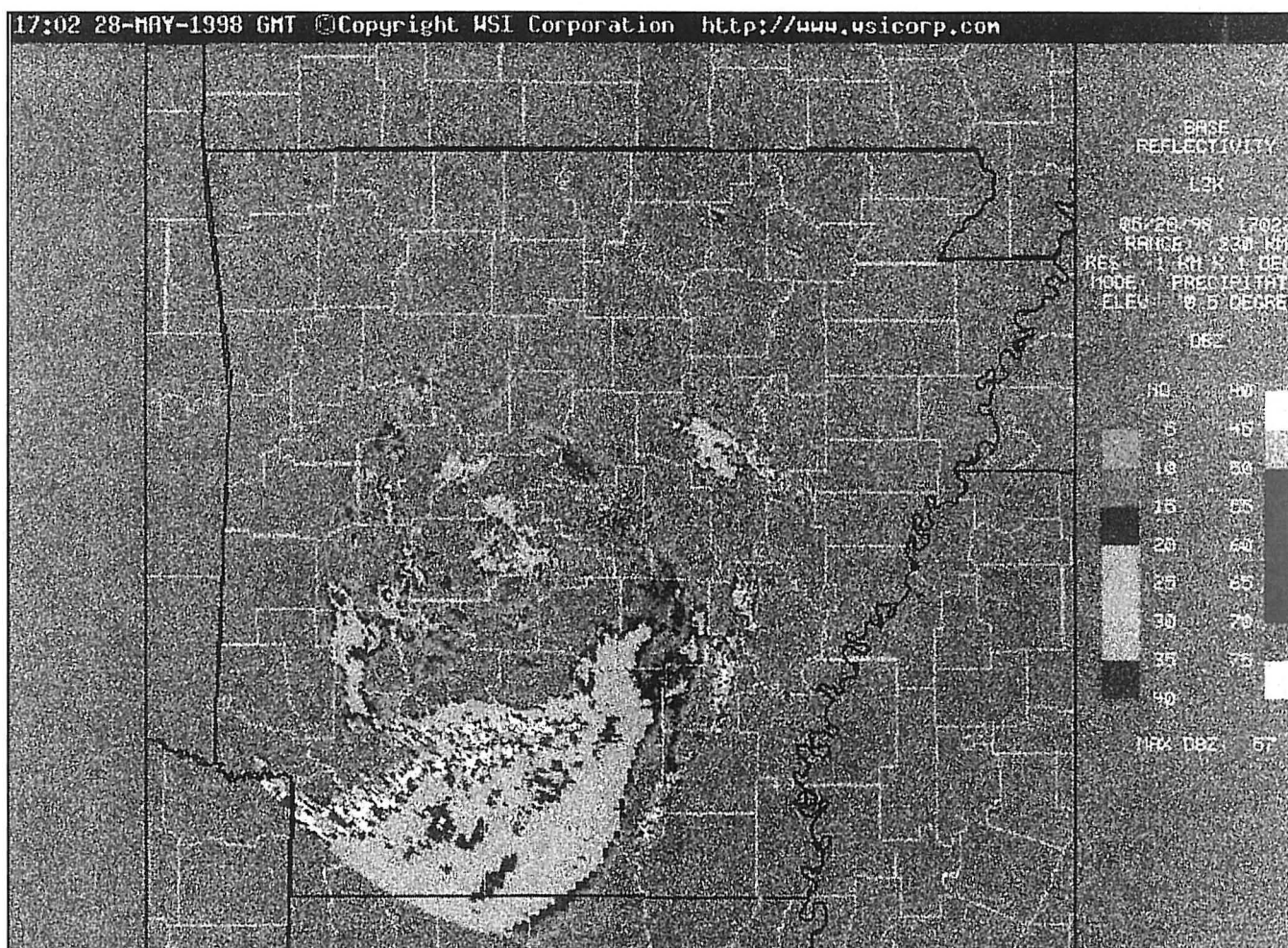


Fig. 4. A WSR-88D reflectivity image from the LIT radar for 1702 UTC 28 May 1998. This image was obtained from WSI Corporation (www.wsicorp.com) and reprinted with their permission.

relatively weak, as this event occurred within a large-scale ridge (Fig. 3).

However, there is evidence of a closed cyclonic circulation over the Arkansas region in the 500-hPa observations (Fig. 3a). There is also evidence of anticyclonic outflow over the same region at 300 hPa. This suggests that the MCV is a warm-core disturbance (e.g., Bartels and Maddox 1991). However, given the horizontal resolution of the rawinsonde temperature observations, it is difficult to verify this warm-core structure. The Day-1 Convective Outlook from the NOAA/NWS/NCEP/Storm Prediction Center (SPC)⁴ valid 1500 UTC 28 May discusses this feature as a warm-core structure. This conclusion can be deduced from Fig. 3 using basic thermal wind arguments (e.g., Bluestein 1992, pp. 187-190). Thus, despite the small-scale occurrence of this event, geostrophic balance arguments can be used appropriately (e.g., Zhang and Fritsch 1988). Finally, as in the MF89 case, the Eta analyses showed that there was a region of strong low-level equivalent potential temperature (θ_e) advection over

Texas (not shown here) indicating the presence of copious amounts of moisture moving northward from the Gulf of Mexico. This is an important ingredient for MCC formation, primarily due to the rapid destabilization of the atmosphere.

While the forecasting of MCC events has been much improved recently, MCCs and associated resulting MCVs can still be a challenging element of the local weather forecast. On Wednesday 27 May, precipitation was forecast for much of western and central Arkansas for Thursday. The outlook from the SPC for the lower Mississippi River Valley indicated that severe thunderstorms were possible over the region in association with the presence of the MCV, especially over Arkansas. Figure 4 shows the radar image from Little Rock (LIT), Arkansas at 1702 UTC 28 May 1998. There is some evidence of cyclonic rotation in the rain bands over central Arkansas and it would appear that the MCV center was just southwest of LIT at this time. However, the heaviest thunderstorms are in the southwest quadrant of the MCV. Some severe weather did occur in association with this event. Nickel and dime-sized hail were reported at Waldo and Texarkana, Arkansas, respectively. High wind gusts (exceeding 58 mph) were observed at this time in

⁴The Day-1 Convective Outlook is obtained from the Storm Prediction Center on the Internet at www.spc.noaa.gov.

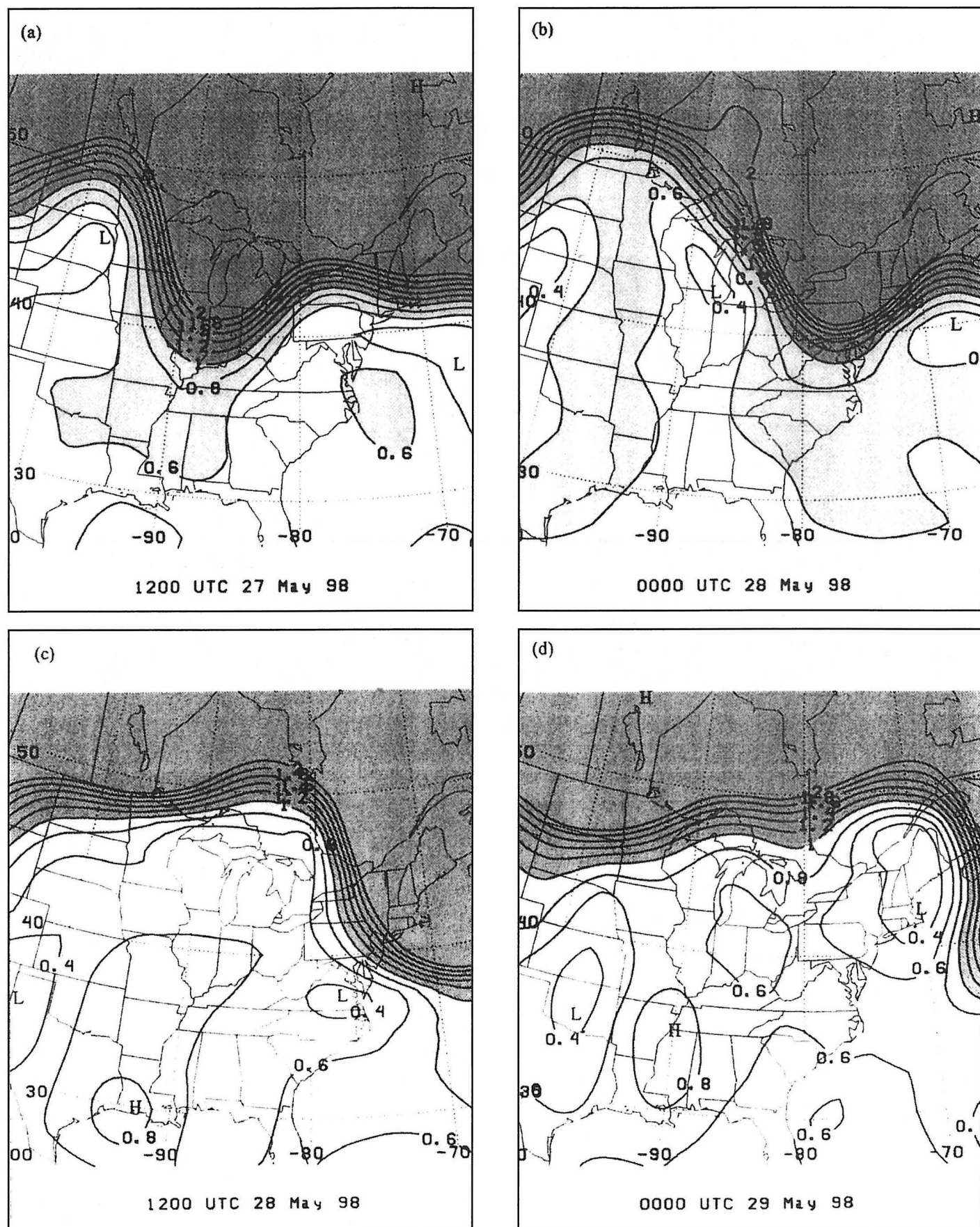


Fig. 5. The 330K potential vorticity field for a) 1200 UTC 27 May 1998, b) 0000 UTC 28 May 1998, c) 1200 UTC 28 May 1998, and d) 0000 UTC 29 May 1998. The increment is 0.2 PVU. Values larger than 1.0 (0.6) PVU are darkly (lightly) shaded.

association with the storms over southwest Arkansas. There was also heavy rain that caused isolated incidents of street flooding over the southern two thirds of Arkansas. Rainfall amounts (24-hour totals) were generally greater than 0.5 inches over the affected area, including 1.56 inches at Hot Springs, Arkansas, and an extreme rainfall total of 12.55 inches at Garland City, Arkansas.

4. Dynamic Analysis

Several studies have shown (e.g., Bartels and Maddox 1991) that MCVs are generated in association with MCSs in a weakly sheared environment, and are also associated with the presence of a pre-existing vortex. Velasco and Fritsch (1987) also demonstrate that the mid-level circulation is what characterizes an MCC, and that the dynamics at these levels are important. An examination of the 500 hPa and 300 hPa maps, as discussed above, shows this weakly sheared environment associated with the ridge over the Southern Plains between 1200 UTC 26 May and 0000 UTC 29 May. Maps of PV on the 330 K potential temperature surface (Fig. 5) covering the development phase of the MCV demonstrate that there was a ribbon of higher PV values over the Midwest at 0000 UTC 28 May (Fig. 5b). By 1200 UTC 28 May, this structure appears as a coherent vortex near the Gulf coast. The 330 K PV field tends to be regarded as an upper tropospheric surface in the mid-latitudes, and demonstrates the PV values in the region of the vortex are characteristic of tropospheric values (usually less than 1 PVU). These maps show that a PV maximum is found concurrent with the MCV, which is additional evidence for the presence of a pre-existing vorticity maximum (also evident in the mid-level height and wind fields at 1200 UTC 26 and 27 May (not shown)).

Thus, it would be instructive to examine middle- and upper-level PV maps (500 hPa to 300 hPa) to locate a strong contribution associated with deep convection due to diabatic heating. We chose to use integrated 500 hPa to 300 hPa potential vorticity, a technique used by Bosart and Lackmann (1995). They used the integrated 850 hPa - 700 hPa PV to study the re-intensification of the vortex associated with Hurricane David into an extratropical cyclone. In this study, we used the integrated vorticity values to examine PV values derived from the NCEP re-analyses, and layer mean PV to examine the Eta initial fields. The layer-mean PV analysis should provide a similar result to the integrated PV values and was chosen since the Eta fields were displayed using the PCGRIDDS visualization software package⁵. Examination of the layer mean 500 - 300 hPa PV field (Fig. 6) demonstrates that the vortex associated with the MCS does intensify

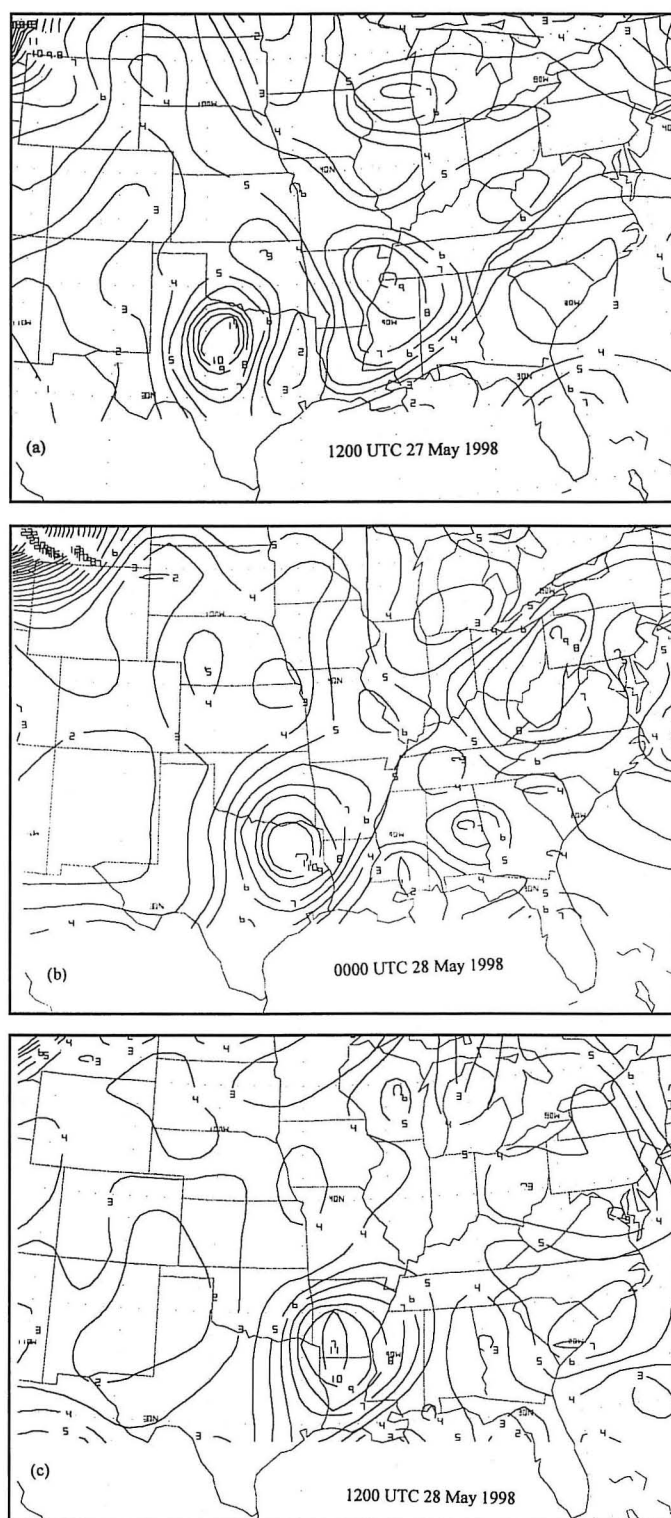


Fig. 6. As in Fig. 5 except the quantity is the 500 - 300 hPa integrated PV (PVU) values using Eta model initial fields. The PV values are shown in 0.1 PVU and the increment is also 0.1 PVU.

within the period 1200 UTC 27 May to 1200 UTC 29 May, as the area encompassed by 0.9 PVU expands during the first 12-h period.

In order to determine whether or not this PV intensification is due to conservative forcing (e.g., vorticity advection, temperature advection) and/or diabatic heat-

⁵The PCGRIDDS macro used to calculate layer mean Potential Vorticity was provided by Dr. James Moore of Saint Louis University and was written by Eric Thaler of the NWS Forecast Office in Denver, Colorado. Layer mean potential Vorticity should provide a qualitatively similar value to the integrated PV provided the profile changes linearly with height. If the level increment equals the averaging layer, then a layer mean quantity is equal to the integrated quantity.

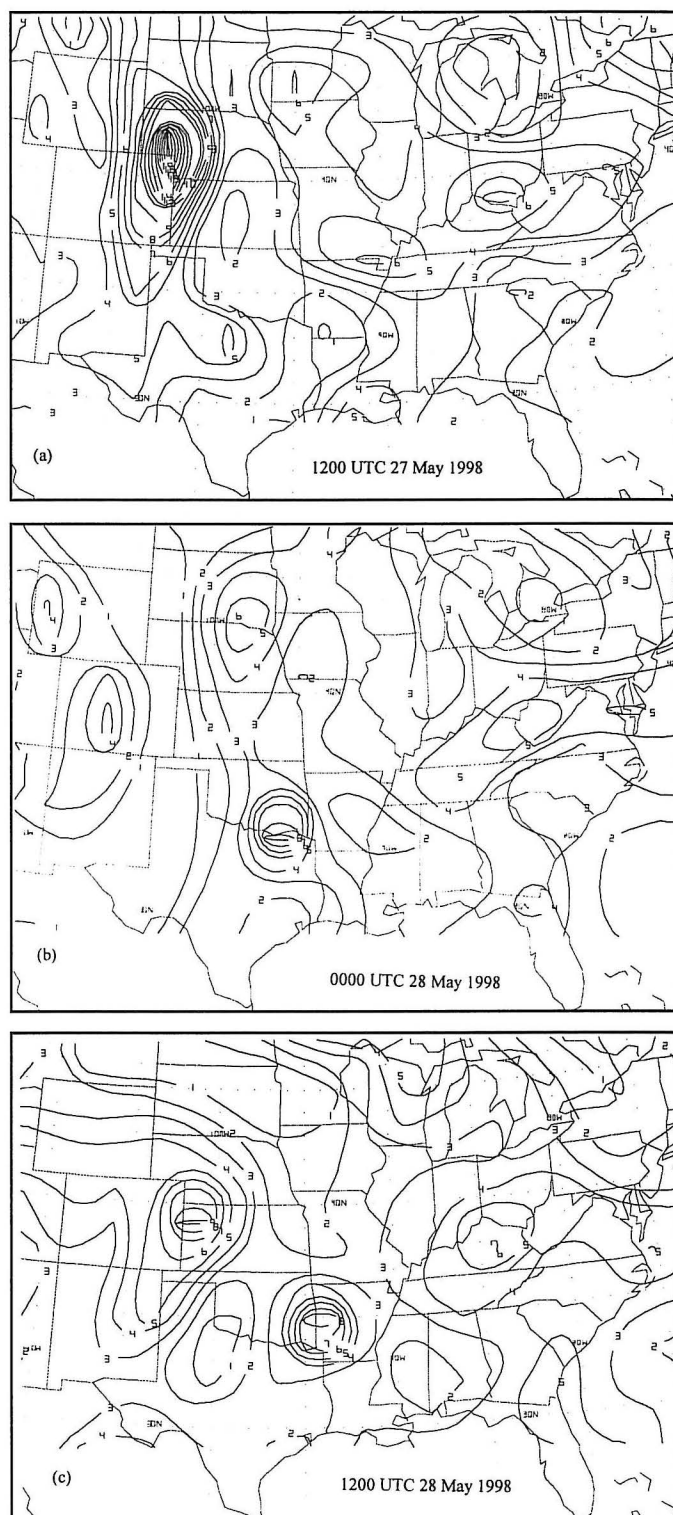


Fig. 7. As in Fig. 6 except the quantity is the 850 - 700 hPa integrated PV (PVU) values using Eta model initial fields.

ing, which is a non-conservative forcing mechanism or a source/sink of PV, a simple PV budget calculation was performed. If PV is conserved, the rate of change in PV should be equal to the advection of PV. At the center point, the advection term in a symmetric vortex is zero. Thus, the local rate of change in the center point PV, the develop-

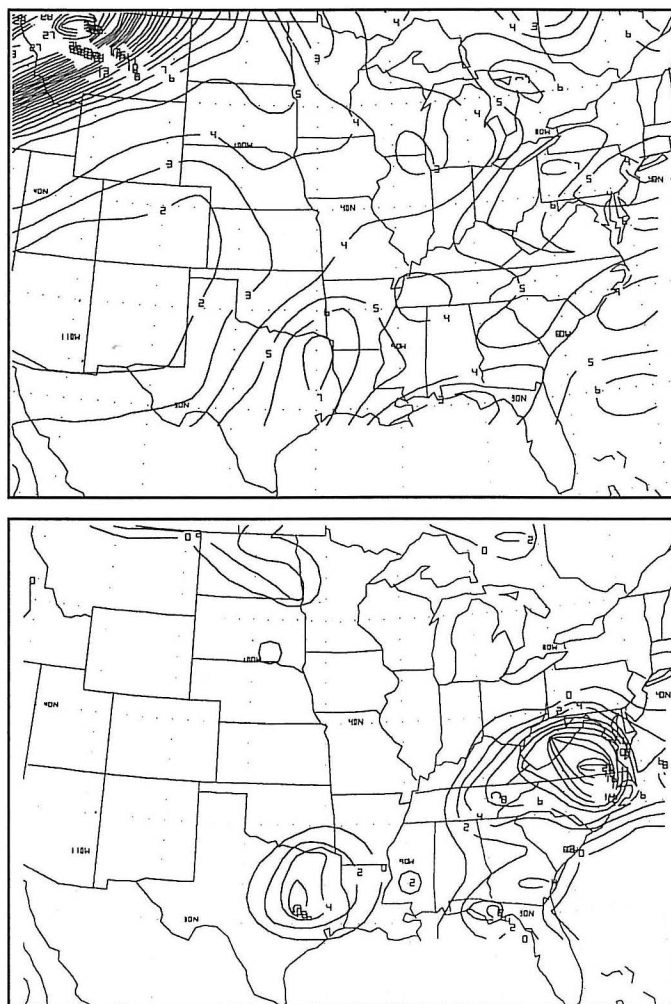


Fig. 8. The a) 24-h forecast 500 - 300 hPa integrated PV for 0000Z 28 May 1998 as in Fig. 6, and the b) 24-h forecast convective precipitation amount (mm, contour interval 2 mm).

ment quantity, should be about equal to the diabatic heating (or generation and destruction of PV). It should be cautioned, however, that these calculations were performed on pressure surfaces, in which case PV is only quasi-conserved (e.g., Bosart and Lackmann 1995; Lupo and Bosart 1999). The five-point grid box centered on the vortex center in the 12-h intervals starting at 1200 UTC 27 May and 0000 UTC 28 May was calculated and compared for both layer mean upper tropospheric (500 - 300 hPa) and lower tropospheric (850 - 700 hPa) PV (Fig. 7). This analysis reveals that the five-point-averaged PV increased by 0.049 PVU (0.208 PVU) in the upper (lower) troposphere for the period 1200 UTC 27 May 1998 - 0000 UTC 28 May 1998. For comparison with the coarser resolution data set, the integrated 500 hPa to 300 hPa PV increase at the center point using the NCEP re-analyses was 0.08 PVU for the same time period. There was no appreciable change in either quantity during the period 0000 UTC 28 May 1998 - 1200 UTC 28 May 1998. During the earlier time period, the low-level increase of 0.208 PVU (48% increase in PV) likely represents development due to latent heat release resulting from the convection associated with the MCV, since other non-conservative effects would be expected to be neg-

ligible in the free atmosphere. The upper level increase (0.049 PVU or a 5% increase) is not as impressive a development, but is nonetheless significant since PV destruction (of equal and opposite sign) should be found above a low-level diabatic heating maximum in the absence of heating/cooling at other levels. Thus, it is possible that the real contribution due to upper-level diabatic heating may be greater than that calculated using this simple technique in order to balance out PV destruction induced by low-level latent heat release. This diabatic heating in the upper layer may be due to the strong convection associated with the MCV in the region. Zhang and Fritsch (1988) and Bartels and Maddox (1991) suggest that heating associated with virtual temperature increases at these levels (maximizing at 400 hPa or higher in Bartels and Maddox 1991), as the column of air moistens and latent heat is released from the rising parcels, could be partially responsible for vorticity generation associated with MCVs. Thus, latent heat release cannot be ruled out as a contributor in generating PV in the middle levels during that time, especially if the convection is sufficiently deep. Nonetheless, numerous studies of larger-scale cyclones show that latent heat release aloft (e.g., Lupo et al. 1992) can supplement the development of the surface feature. Thus, we propose that a similar mechanism partially led to the strengthening of the mid-level vortex (see Figs. 5 and 6), which also expanded in area.

Also, note that the strongest layer mean PV values during the 12-h from 0000 UTC 28 May to 1200 UTC 28 May are close to the southwest quadrant of the MCV, which is where the strongest convection was located. Most severe weather and heavy rain reports occurred across southern Arkansas during the 12-h following 1200 UTC 28 May. Thus, the 500-300 hPa integrated PV may have usefulness as an operational forecasting tool since mid-level PV generation due to diabatic heating may be indicative of deep convection.

To demonstrate the utility of integrated 500 - 300 hPa PV, Eta model forecast fields of this quantity and precipitation are examined. Figure 8a shows the 24-h forecast integrated PV valid for 0000Z 28 May 1998. While the intensity of the upper air feature was weaker than the observed (see Fig. 6b), the location was well forecast and the forecast convective precipitation shield (which was 100% of the total forecast precipitation) (Fig. 8b) was nearly co-located of the upper-level integrated PV values. The forecast precipitation maximum is just to the southwest of the forecast PV maximum. By comparison, the integrated 850-700 hPa PV maximum was forecast to be located north of the integrated 500-300 hPa PV maximum. This map is not shown here since the 850-700 hPa PV field was well forecast (compares to Fig. 7b in strength and location). Thus, the value of the technique as a forecasting tool may at least partially lie in inferring the likelihood of future convection. However, more studies would be needed to verify this assertion.

5. Conclusions

The occurrence of an unusually large and long-lived MCV event was discussed using data and products obtained from the Internet and the NCEP re-analyses.

This MCV event did not generate very many reports of severe weather over the Southern Plains states, although there was heavy precipitation observed over central and southern Arkansas on 28 May 1998. The amounts were generally 0.5 inches or greater (Shreveport, LA Weather Service Office, personal communication, 1998) including 1.56 inches at Hot Springs, and an extreme report of 12.55 inches at Garland City, Arkansas. A synoptic analysis of the environment in which this MCV event developed shared many characteristics in common with that of a similar MCV event analyzed by MF89. However, this event exhibited more eastward movement than the MF89 MCV. Also, this event occurred well within a large-scale ridge located over the eastern two thirds of the United States.

A dynamical analysis demonstrates that, as other studies have shown, this MCV event develops within a weakly sheared environment. Also, it is shown that there was a pre-existing PV maximum associated with the MCV, which has also been demonstrated by other investigators. This study shows that the 500 - 300 hPa vortex strengthens due to diabatic heating (latent heat release) as demonstrated by the integrated values. Finally, it is also shown that higher values of 500 - 300 hPa integrated or layer-mean PV values were associated with the most severe weather and rainfall, and may have value as an operational forecasting tool.

Acknowledgments

The authors would especially like to thank Mr. Steve Keighton and Dr. John Nielsen-Gammon for their comments on this work. The authors would also like to thank the staff at the National Weather Service Forecast Office (NWSFO) Shreveport, Louisiana, for providing information about heavy rainfall totals and severe weather reports associated with the MCV for 28 May 1998. Finally, we would like to thank Scott Truett and Ron Przybylinski from NWSFO Saint Charles, Missouri, for providing the Eta model initializations used in this study, and Dr. James Moore at Saint Louis University for providing the PCGRIDDS software and macros (written by Eric Thaler at NWSFO Denver, Colorado).

References

- Bartels, D. L., and R.A. Maddox, 1991: Mid-level cyclonic vortices generated by mesoscale convective systems. *Mon. Wea. Rev.*, 119, 104-118.
- Bluestein, H.B., 1992: *Synoptic and Dynamic Meteorology in the Mid-latitudes. Vol. I: Principles of Kinematics and Dynamics*. Oxford University Press, 431 pp.
- Bosart, L.F., and G.M. Lackmann, 1995: Post-landfall tropical cyclone reintensification in a weakly barotropic environment: A case study of Hurricane David (September 1979). *Mon. Wea. Rev.*, 123, 3268-3291.
- Businger, J. A., and R.J. Reed, 1989: Polar Lows. *Polar and Antarctic Lows*, P.F. Twitchell, E.A. Rasmussen, and K.L. Davidson, and A. Deepak, Eds., 3-45.

- de Coning, E, G.S. Forbes, and E. Poolman, 1998: Heavy precipitation and flooding on 12-14 February 1996 over the summer rainfall regions of South Africa: Synoptic and isentropic analysis. *Natl. Wea. Dig.*, 22:3, 25-36.
- Ertel, H., 1942: Ein neuer hydrodynamischer. *Wirbesatz. Meteorol. Z.*, 59, 277-281.
- Gallee, H., 1995: Simulation of the mesocyclonic activity in the Ross Sea, Antarctica. *Mon. Wea. Rev.*, 123, 2051-2069.
- Hoskins, B.J., M.E. McIntyre, and A.W. Robertson, 1985: On the use and significance of isentropic potential vorticity maps. *Quart. J. Roy. Met. Soc.*, 111, 877-946.
- _____, and P. Berrisford, 1988: A potential vorticity perspective of the storm of 15 – 16 October 1987. *Weather*, 43, 122-129.
- Johnston, E.C., 1981: *Mesoscale vorticity centers induced by mesoscale convective complexes*. Master's thesis. University of Wisconsin-Madison, 54 pp.
- Kalnay, E., M. Kanamitsu, R. Kistler, W. Collins, D. Deaven, L. Gandin, M. Iredell, S. Saha, G. White, J. Woolen, Y. Zhu, M. Chelliah, W. Ebisuzaki, W. Higgins, J. Janowiak, K.C. Mo, C. Ropelowski, J. Wang, A. Leetmaa, R. Reynolds, R. Jenne, and D. Joseph, 1996: The NCEP/NCAR 40-year reanalysis project. *Bull. Amer. Met. Soc.*, 77, 437-471.
- Levinson, D.H., and R.M. Banta, 1995: Observations of a terrain-forced mesoscale vortex and canyon drainage flows along the front range of Colorado. *Mon. Wea. Rev.*, 123, 2029-2050.
- Lupo, A.R., P.J. Smith, and P. Zwack, 1992: A diagnosis of the explosive development of two extratropical cyclones. *Mon. Wea. Rev.*, 120, 1490-1523.
- _____, and L.F. Bosart, 1999: An analysis of a relatively rare case of continental blocking. *Quart. J. Roy. Meteor. Soc.*, 125, 107-138.
- Maddox, R.A., 1980 Mesoscale convective complexes. *Bull. Amer. Meteor. Soc.*, 61, 1374-1387.
- _____, K.W. Howard, D.L. Bartels, D.M. Rodgers, 1986: Mesoscale convective complexes in the middle latitudes, *Mesoscale Meteorology and Forecasting*, Peter S. Ray, Editor, 390-413, Published by: American Meteorological Society, 793 pp.
- Menard, R.D., and J. M. Fritsch, 1989: A mesoscale convective complex-generated inertially stable warm core vortex. *Mon. Wea. Rev.*, 117, 1237-1261.
- Moore, J.T., 1993: *Isentropic analysis and interpretation: Operational applications to synoptic and mesoscale forecast problems*. National Weather Service Training Center, Kansas City, MO, 99 pp.
- Nielsen-Gammon, J.W., and R.J. Lefevre, 1996: Piecewise tendency diagnosis of dynamical processes governing the development of an upper-tropospheric trough. *J. Atmos. Sci.*, 53, 3120-3142.
- Pedlosky, J., 1987: *Geophysical Fluid Dynamics*. 2nd ed., Springer-Verlag, 710 pp.
- Uccellini, L.W., 1976: Operational diagnostic applications of isentropic analysis. *Natl. Wea. Dig.*, 1:1, 4-12.
- Velasco, I., and J.M. Fritsch, 1987: Mesoscale convective complexes in the Americas. *J. Geophys. Res.*, 92, 9591-9613.
- Weisman, M., 1993: The genesis of severe long-lived bow echoes. *J. Atmos. Sci.*, 50, 645-670.
- Zhang, D.L., and J.M. Fritsch, 1987: Numerical simulation of a meso-scale structure and Evolution of the 1977 Johnstown flood. Part II: inertially stable warm-core vortex and the mesoscale convective complex. *J. Atmos. Sci.*, 44, 2593-2612.
- _____, and _____, 1988: A numerical simulation of a convectively generated inertially stable, warm-core extratropical mesovortex over land. Part I: structure and evolution. *Mon. Wea. Rev.*, 116, 2660-2687.
- _____, 1992: The formation of a cooling-induced mesovortex in the trailing stratiform region of a mid-latitude squall line. *Mon. Wea. Rev.*, 120, 2763-2785.